REPORT DOCUMENTATION PAGE

Form Approved
OMB No. 0704-0188

1. AGENCY USE ONLY (Leave blank)	2. REPORT DATE	3. REPORT TYPE AND DATES COVERED
	9/30/96	Final Report; 10/01/91 - 2/28/96

4. TITLE AND SUBTITLE
Dynamic Effects of Suction/Heating on Turbulent Boundary Layers

5. FUNDING NUMBERS
$317,728

6. AUTHOR(S)
Ron Blackwelder

7. PERFORMING ORGANIZATION NAME(S) AND ADDRESS(ES)
Department of Aerospace Engineering
University of Southern California
Los Angeles, CA 90089-1191

8. PERFORMING ORGANIZATION REPORT NUMBER

9. SPONSORING/MONITORING AGENCY NAME(S) AND ADDRESS(ES)
Dr. Pat Purtell, Code 333
Office Of Naval Research
Ballston Tower One
800 North Quincy St.
Arlington, VA 22217-5000

10. SPONSORING/MONITORING AGENCY REPORT NUMBER

11. SUPPLEMENTARY NOTES

12a. DISTRIBUTION/AVAILABILITY STATEMENT
Approved for public release; distribution unlimited

12b. DISTRIBUTION CODE

13. ABSTRACT (Maximum 200 words)

See enclosed report.

14. SUBJECT TERMS	15. NUMBER OF PAGES
turbulence, boundary layers	4
	16. PRICE CODE

17. SECURITY CLASSIFICATION OF REPORT	18. SECURITY CLASSIFICATION OF THIS PAGE	19. SECURITY CLASSIFICATION OF ABSTRACT	20. LIMITATION OF ABSTRACT
Unclassified	Unclassified	Unclassified	UL

GENERAL INSTRUCTIONS FOR COMPLETING SF 298

The Report Documentation Page (RDP) is used in announcing and cataloging reports. It is important that this information be consistent with the rest of the report, particularly the cover and title page. Instructions for filling in each block of the form follow. It is important to ***stay within the lines*** to meet ***optical scanning requirements***.

Block 1. Agency Use Only *(Leave blank)*.

Block 2. Report Date. Full publication date including day, month, and year, if available (e.g. 1 Jan 88). Must cite at least the year.

Block 3. Type of Report and Dates Covered. State whether report is interim, final, etc. If applicable, enter inclusive report dates (e.g. 10 Jun 87 - 30 Jun 88).

Block 4. Title and Subtitle. A title is taken from the part of the report that provides the most meaningful and complete information. When a report is prepared in more than one volume, repeat the primary title, add volume number, and include subtitle for the specific volume. On classified documents enter the title classification in parentheses.

Block 5. Funding Numbers. To include contract and grant numbers; may include program element number(s), project number(s), task number(s), and work unit number(s). Use the following labels:

C	- Contract	PR	- Project
G	- Grant	TA	- Task
PE	- Program Element	WU	- Work Unit Accession No.

Block 6. Author(s). Name(s) of person(s) responsible for writing the report, performing the research, or credited with the content of the report. If editor or compiler, this should follow the name(s).

Block 7. Performing Organization Name(s) and Address(es). Self-explanatory.

Block 8. Performing Organization Report Number. Enter the unique alphanumeric report number(s) assigned by the organization performing the report.

Block 9. Sponsoring/Monitoring Agency Name(s) and Address(es). Self-explanatory.

Block 10. Sponsoring/Monitoring Agency Report Number. *(If known)*

Block 11. Supplementary Notes. Enter information not included elsewhere such as: Prepared in cooperation with...; Trans. of...; To be published in.... When a report is revised, include a statement whether the new report supersedes or supplements the older report.

Block 12a. Distribution/Availability Statement. Denotes public availability or limitations. Cite any availability to the public. Enter additional limitations or special markings in all capitals (e.g. NOFORN, REL, ITAR).

- **DOD** - See DoDD 5230.24, "Distribution Statements on Technical Documents."
- **DOE** - See authorities.
- **NASA** - See Handbook NHB 2200.2.
- **NTIS** - Leave blank.

Block 12b. Distribution Code.

- **DOD** - Leave blank.
- **DOE** - Enter DOE distribution categories from the Standard Distribution for Unclassified Scientific and Technical Reports.
- **NASA** - Leave blank.
- **NTIS** - Leave blank.

Block 13. Abstract. Include a brief *(Maximum 200 words)* factual summary of the most significant information contained in the report.

Block 14. Subject Terms. Keywords or phrases identifying major subjects in the report.

Block 15. Number of Pages. Enter the total number of pages.

Block 16. Price Code. Enter appropriate price code *(NTIS only)*.

Blocks 17. - 19. Security Classifications. Self-explanatory. Enter U.S. Security Classification in accordance with U.S. Security Regulations (i.e., UNCLASSIFIED). If form contains classified information, stamp classification on the top and bottom of the page.

Block 20. Limitation of Abstract. This block must be completed to assign a limitation to the abstract. Enter either UL (unlimited) or SAR (same as report). An entry in this block is necessary if the abstract is to be limited. If blank, the abstract is assumed to be unlimited.

DISCLAIMER NOTICE

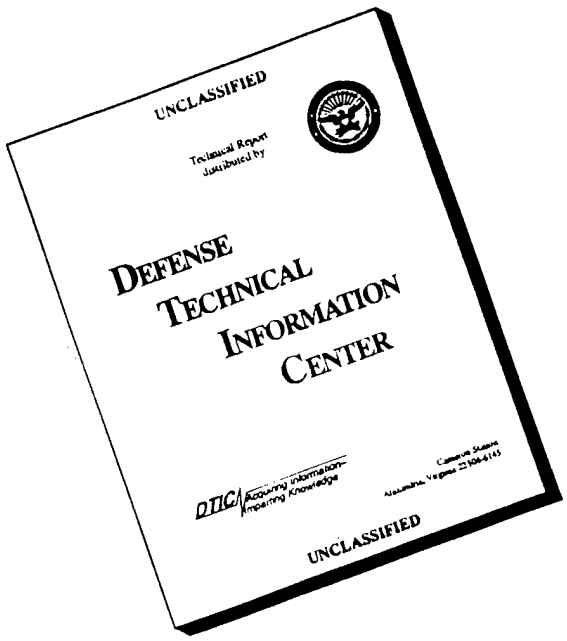

THIS REPORT IS INCOMPLETE BUT IS THE BEST AVAILABLE COPY FURNISHED TO THE CENTER. THERE ARE MULTIPLE MISSING PAGES. ALL ATTEMPTS TO DATE TO OBTAIN THE MISSING PAGES HAVE BEEN UNSUCCESSFUL.

Final Technical Report

"Dynamic Effects of Suction/Heating on Turbulent Boundary Layers"
(Task 1 - Contract N00014-92-J-1062)

10-1-91 to 2-28-96

by

Ron Blackwelder, Principal Investigator
Department of Aerospace Engineering
University of Southern California
Los Angeles, CA 90089-1191

Scientific Officer: Dr. Pat Purtell
Code 1132F

Description of the Scientific Research Goals

The goals of this research were to constructively interact with and alter vortical structures embedded within boundary layers. The concept of selective interaction was developed which utilized information about the location of the vortical structures so that the interaction could be tailored to more efficiently alter the eddies. Different types of mechanisms were deployed to alter the eddies including suction, blowing, actuators, etc. These methods altered the development of streamwise vortices sufficiently that their breakdown and mixing were significantly delayed.

Significant Results Obtained

The experiments in air were all conducted in the University of Southern California Görtler wind tunnel described in detail by Swearingen & Blackwelder (JFM,182,255,1987). The concave test plate has a span of 1.2m, is 2.4m long, and has a radius of curvature of 3.0m. The freestream u' turbulence level was less than 0.07% and spanwise deviations in the free stream velocity along the spanwise direction were less than 0.5% across the test section.

Suction was the first mechanism employed to alter the streamwise vortices. It was applied in an boundary layer consisting of a Görtler instability developing on a concave wall. This flow produces streamwise vortices and elongated low speed regions between them analogous to the low speed streaks in turbulent boundary layers. These emulated streaks are steady and thus pose a more controlled eddy structure than in the turbulent boundary layer. They grow downstream, become unstable and breakup in an analogous fashion to their counterparts in the turbulent boundary layer. Suction was employed through individual holes drilled along streamlines in the spanwise region between two vortices. The hole patterns utilized different diameters and geometrical configurations

on the wall. Air was withdrawn through the holes to provide discrete points of suction. Differing rates of suction through the holes was used to explore the effects upon the eddy structure. Visualization images from a smoke-wire were captured using a video camera and hot-wire data were analyzed to determine the best suction rates.

The principal results from the suction were reported in the attached AIAA Journal article (AIAA J, vol 33, 1076, 1995). The suction significantly delayed the development of the low speed regions and their breakdown. The amount of suction required was quite small; being an order of magnitude smaller than that required for the asymptotic suction profile. It was applied through a finite number of discrete holes to keep the velocity through the hole sufficiently small. For larger suction rates, the velocity through the suction holes was sufficiently large that it promoted an additional instability along the low speed streaks. Streamwise slits would provide better results. Nevertheless, the suction delayed the breakdown of the low speed region by 10 to 20 boundary layer thicknesses downstream. By analogy, it should reduce the production of turbulent energy in a turbulent boundary layer.

A second mechanism for interacting with the streamwise vortices consisted of a small delta wing made of spring steel. The leading edge of the wings were swept approximately 75° back from the mean flow. Various geometries were studied and its length scales were optimized to interact with the pre-existing streamwise vortices. Typically the delta wings had a chord of 30-44 mm and a thickness of 0.1mm. Their spanwise length of 22 mm was approximately the distance between the naturally occurring stationary Görtler vortices. The delta wings were mounted flush with the wall at various streamwise locations from the leading edge. The trailing edge of the wing was always in contact with the wall and the oscillation provided an unsteady angle of attack. The wing was placed at various locations with respect to the low speed regions. Its orientation with respect to the low speed regions was found to be a critical parameter in the study as discussed later. The actuator was oscillated with amplitudes between zero and five viscous scale heights and at frequencies between 20 and 400 Hz; i.e. $.005 < f \cdot \nu/u_\tau^2 < 0.1$. Initially the delta wing was driven by an acoustic speaker, but later results were obtained using a piezo-ceramic bimorph located on the flush mounted region of the wing. The streamwise velocity was measured by rakes of hot-wires in the normal and spanwise directions located downstream of the actuator on the concave wall. In addition, a smoke wire was used to visualize the low speed streaks and their subsequent breakdown. Some of the main results were reported in ASME FED-Vol 193 on Turbulence Control(see attached paper).

The results of the perturbation were striking. The smoke visualization indicated that the breakdown of the low speed region between the streamwise vortices was delayed by 10 to 20 boundary layer thicknesses depending upon the amplitude and frequency of the delta wing. This was verified by the velocity measurements. When the actuator was properly orientated, the velocity deficit in the low speed region was always reduced by the excitation. Not only was the deficit reduced, but the spatial extent of the strong spanwise shear was reduced as well. This appeared to be the key element of the control; i.e. the strength of the spanwise shear was reduced thus delaying the secondary instability that led to the breakdown. With oscillation amplitudes of one viscous scale, the streamwise velocity fluctuations at the control location downstream had a corresponding decrease of approximately 50%. Thus it is clear that only a very small amplitude oscillation in the wall region is sufficient to have a strong and profound effect on the transitional boundary layers.

The vortices ultimately broke down further downstream. This was found to be due to an inviscid instability that developed on the shear in the vertical direction. Thus although the spanwise shear was reduced, the vertical shear increased and it was believed that this was the reason that the low speed region ultimately broke down in the excited case. It was also observed that the breakdown location was a strong nonlinear function of the excitation amplitude. It was suspected that the movement and strength of the disturbance vortices must depend upon their relative location with respect to the original Görtler vortices. This may help explain the non-linearity encountered in the amplitude of the disturbance.

List of Publications

Papers Published in Refereed Journals:

"Vortex Generators used to Control Laminar Separation Bubbles," with M. Kerho (undergraduate student), S. Hutcherson (undergraduate student), and R. Liebeck (faculty), Journal of Aircraft, vol. 30, 315, 1993.

"An Experimental Study of Receptivity of Acoustic Waves in Laminar Boundary Layers," with M.D. Zhou and D. Liu (graduate student) and Ron F. Blackwelder, Experiments in Fluids, vol. 17, 129, 1994.

"The Role of the Outer Region in Turbulent Boundary Layer Bursting Process," R. Myose (graduate student) and Ron F. Blackwelder, Journal of Fluid Mechanics, vol. 259, 345, 1994.

Invited Presentations:

"Initiation of Turbulent Spots in a Laminar Boundary Layer by Rigid Particulates," with F.K. Browand, C. Fisher, and P. Taniguchi, End-Stage Transition Workshop, Syracuse University, Aug. 1993.

"Delay of Break-Down of Streamwise Vortices embedded in a Boundary Layer," D. Liu (graduate student) and Ron F. Blackwelder, ASME Fluid Mechanics Conference, Lake Tahoe, CA, June 21-24, 1994.

"Modification of Near-Wall Mixing Using Small Delta Wing Actuators," R.F. Blackwelder and D. Lui, AIChE Annual Meeting, November 13-18, 1994, San Francisco, CA. (invited talk)

Other Presentations:

"Transient Energy Release Pressure Driven Microactuators for Control of Wall-Bounded Turbulent Flows," with D.C. Wadsworth, E.P. Muntz, and G.R. Shiflett, AIAA-93-3271, AIAA Shear Flow

Conference, Orlando, FL, July 6-9,1993.

"Initiation of Turbulent Spots in a Laminar Boundary Layer by Rigid Particulates," with F.K. Browand, C. Fisher, and P. Taniguchi, Am. Physical Society, Fluid Dynamics Meeting, Tallahassee, Nov. 1992.

"Selective Suction for Controlling the Breakdown of Streamwise Vortices on Concave Walls," Roy Myose and Ron F. Blackwelder, AIAA-94-2216, AIAA Fluid Dynamics Conference, Colorado Springs, CO, June 20-23, 1994.

"A Correlation for Transition at R=1 Using an Integral Disturbance Energy Scale," P. LeBlanc, Ron F. Blackwelder and R.H. Liebeck, Am. Physical Society, Fluid Dynamics Meeting, Albuquerque, NM, Nov. 1993.

"Manipulation of Streamwise Vortices in a Boundary Layer by a Piezoceramic Actuator," D.Liu and R.F. Blackwelder, American Physical Society, Fluid Dynamics Division, Atlanta, GA, November 20-22, 1994.

Technology Transfer

The Naval Underwater Systems Center, New London, has utilized some of the information obtained from our study of initiation of turbulent patches by particulates in a laminar boundary layer. This laboratory help initiate this research and funded its during its first two years.

Dr. Don McEligot at the Idaho National Engineering Laboratory, Idaho Falls, ID, has utilized the algorithm developed several years ago for the detection of bursts in the near-wall region of a bounded turbulent shear flow.

Dr. Carl Friehe at the University of California at Irvine has utilized simultaneous streamwise velocity data and algorithms developed under ONR support for the detection of bursts in the turbulent boundary layers.

AIAA JOURNAL
Vol. 33, No. 6, June 1995

Control of Streamwise Vortices Using Selective Suction

Roy Y. Myose*
Wichita State University, Wichita, Kansas 67260-0044
and
Ron F. Blackwelder†
University of Southern California, Los Angeles, Los Angeles, California 90089-1191

The breakdown of streamwise vortices was controlled using selective suction. A Görtler flowfield was used to produce streamwise vortices emulating turbulent boundary-layer eddies in a steady laminar-like environment. Suction was applied at single locations under the low-speed region between counter-rotating vortex pairs. A suction coefficient two orders of magnitude less than that required for an asymptotic profile was sufficient to significantly delay the breakdown of the vortices. At high-suction rate, however, premature breakdown resulted due to the creation of an additional instability in the spanwise direction. Results suggest that an ideal control method should produce fuller profiles in the normal direction and eliminate the difference between low- and high-speed regions in the spanwise direction.

Nomenclature

A_E	= effective suction area
A_S	= suction area
C_S	= suction coefficient, $Q_S/(A_E U_\infty)$
Q_S	= volumetric flow rate of suction
U_∞	= freestream velocity
V_W	= velocity through wall, Q_S/A_S
x, y, z	= streamwise, normal, and spanwise distance
δ	= boundary-layer thickness

Introduction

SUCTION has been used to manipulate and control boundary layers in many diverse conditions ranging from the delay of transition to the removal of turbulent boundary layers. During the 1960s, test flights of the X-21 aircraft demonstrated the feasibility of maintaining laminar flow over the wing using suction through many small spanwise slots.[1] Recent test flights of a modified F-16XL aircraft using suction through a wing glove to maintain laminar flow suggests a drag reduction on the order of about 8%.

In the past, suction and other control methods have been utilized over entire surfaces without regards to the structure of the boundary layer. That is, the suction has been applied as uniformly as possible over the entire surface. This alters the mean velocity uniformly and gives it a fuller profile. Such profiles (known as the asymptotic suction profile) are more stable and produce a higher critical Reynolds number.[2] Thus, this technique is useful for delaying transition and reducing the overall drag of a body. The fuller profile produces a larger shear stress at the wall which increases the laminar skin friction. However, if the suction can maintain a laminar flow, the skin friction is less than the turbulent case, and the overall drag is reduced. In the turbulent boundary layer, uniform suction and the fuller profile associated with it will always produce a larger shear stress and, hence, increase the drag.

The novel aspect of the present experiment is that the suction (i.e., the control method) is employed selectively. That is, the control is not applied uniformly over the entire flowfield, but, instead, is designed to act selectively on the identifiable eddies (e.g., low-speed streaks). In turbulent bounded shear flows, the growth and breakdown of low-speed streaks are closely associated with the bursting process.[3,4] This method, therefore, requires some advanced knowledge about the eddies themselves (e.g., their location) along with some knowledge of their dynamics. Given such information, the suction can be employed beneficially to interfere with the growth and movement of the eddies and thus interrupt the Reynolds stress production.[5]

Johansen and Smith[6] used small longitudinal cylinders to anchor meandering low-speed streaks to known locations. Roon and Blackwelder[7] used these longitudinal roughness elements combined with suction (selectively) at the wall underneath the same spanwise location as the low-speed streak and found that the number and duration of low-speed streaks decreased. Gad-el-Hak and Blackwelder[8] artificially generated single and periodic hairpin eddies in a laminar boundary layer, and then used a streamwise oriented suction slot to successfully eliminate this hairpin eddy.

In the present experiment, selective suction was employed in an emulated boundary layer to test its effects in a controlled environment. This differs from the turbulent boundary layer used by Roon and Blackwelder[7] (which involves streak identification issues) or the solitary artificially generated structure utilized by Gad-el-Hak and Blackwelder[8] (as opposed to multiple streaks spatially offset in the spanwise direction). The present emulated boundary layer consists of a Görlter instability developing on a concave wall. Swearingen and Blackwelder[4] have shown that the resulting weak streamwise vortices produce elongated low-speed regions analogous to low-speed streaks in turbulent boundary layers. These emulated streaks are steady and, thus, provide a more controlled eddy structure than in the turbulent boundary layer; at the same time, they have normalized scales comparable to the turbulent boundary-layer structure. As the emulated streaks grow downstream, they become unstable and breakdown in a fashion analogous to their counterpart in the turbulent boundary layer. The present experiment also differs from the previous experiments in that suction was applied pointwise through single holes (which would have practical design advantages) rather than a streamwise oriented slot.

Experimental Method

The experiment was conducted in the low-turbulence open return wind tunnel shown schematically in Fig. 1. The test section is 245 cm long in x with a 15 cm in y by 120 cm in z cross section and a 320 cm radius of curvature concave test wall. Detail A of

Received April 6, 1994; presented as Paper 94-2216 at the AIAA 25th Fluid Dynamics Conference, Colorado Springs, CO, June 20–23, 1994; revision received Oct. 19, 1994; accepted for publication Oct. 19, 1994.

*Assistant Professor, Department of Aerospace Engineering. Senior Member AIAA.
†Professor, Department of Aerospace Engineering. Associate Fellow AIAA.

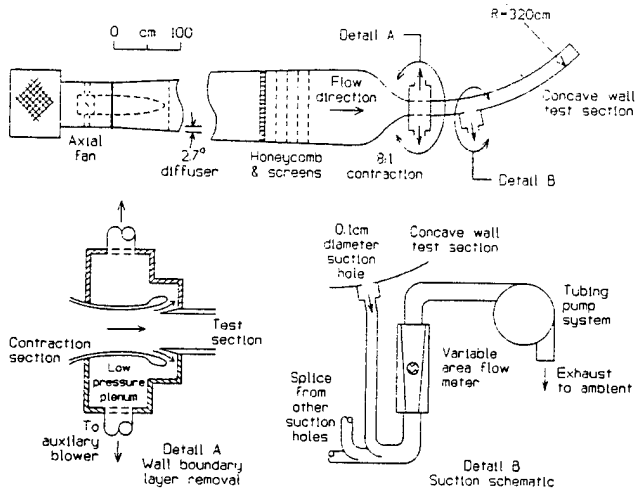

Fig. 1 Experimental setup.

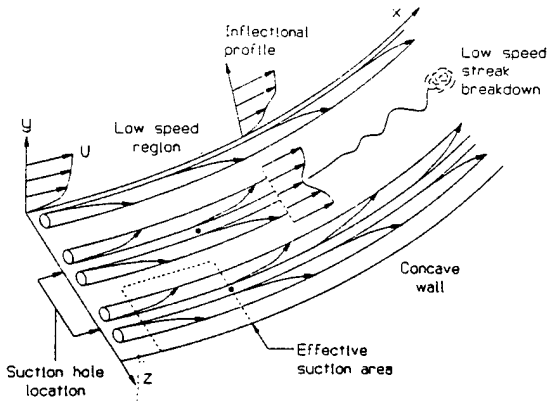

Fig. 2 Experimental situation: uppermost vortex shows inflectional velocity profile, center vortex pair shows inflectional profile in the spanwise direction and development and breakdown of low-speed streak, lowermost vortex pair shows effective suction area. Two of the nine suction holes (depicted by •), each of which is located under the low-speed streak, are shown. Scale in the streamwise x direction is compressed relative to the other directions.

Fig. 1 shows the wall boundary-layer removal device which is used to tangentially remove the tunnel side wall boundary layer. This ensures that the origin of the test section boundary layer begins at the concave wall leading edge. The change in pressure coefficient in the wind tunnel is $\delta(dc_p/dx) \approx -3 \times 10^{-2}$ for $x \geq 70$ cm (i.e., where the measurements were taken). Thus, the pressure gradient is constant and slightly favorably. Additional details of the wind tunnel are given by Swearingen and Blackwelder.[4] A pitot-static tube and pressure transducer system was used to maintain a freestream velocity of $U_\infty = 500$ cm/s ±1% throughout the course of this experiment.

Suction was applied pointwise at $x = 40$ cm through nine individual 0.1-cm-diam holes located at nine different spanwise positions between counter-rotating streamwise vortex pairs (i.e., under the low-speed regions) as depicted in Fig. 2. Air was sucked out of the individual holes via Tygon tubing/Masterflex tubing pump system as shown in detail B of Fig. 1. The suction flow rate was measured by a variable area flow meter. Varying suction rates were applied to explore their effect on the eddy structure. A sheet of smoke was introduced at $x = 22$ cm and $y = 0.14$ cm ($y/\delta_{Blasius} \approx 0.35$) using the smoke-wire technique.[4] The resulting smoke patterns were then recorded using a charge coupled device (CCD) camera and super-video home system (S-VHS) video system. Streamwise velocity measurements were taken under select conditions by traversing a single sensor hot wire. The standard hot-wire measurement technique[4] was used in this experiment.

The amount of applied suction is defined by the suction coefficient $C_S \equiv V_W/U_\infty$ where V_W is the normal velocity through the wall.[2] In the case of uniform suction, the normal velocity through the wall is then given by $V_W = Q_S/A_S$ where Q_S is the volumetric flow rate of suction and A_S is the applied suction area. Since suction is applied under a very large area in this case, the average velocity through the wall is rather small. In the case of pointwise suction utilized in this experiment, the associated volumetric flow rate is relatively small. However, the velocity through the wall is relatively large due to the fact that suction is applied at a single point through a small hole area. To allow comparison with uniform suction, especially the asymptotic suction profile case, the suction coefficient is defined as $C_S = Q_S/(A_E \cdot U_\infty)$ where A_E is the area over which the suction has an effect. There are two possible schemes for characterizing this effective area. One scheme is to determine the downstream area which the suction affects. This would require determining the downstream location where low-speed streaks break down with and without suction. The region of downstream delay in breakdown would then be used as the effective area. However, it would then be difficult to ascribe a suction coefficient for a case with no delay (i.e., an effective area of zero) as well as cases involving early breakdown. Since the low-speed streak undergoes growth, another scheme for characterizing the effective area is to view the role of suction as reversing (or reducing) the effects of this growth which occurred upstream. This second scheme, as described subsequently, was chosen for the purposes of comparison with the asymptotic suction case.

Although the instability responsible for developing the vortical system in Görtler flow commences close to the leading edge, a small streamwise distance is required before its effect is noticeable. According to Swearingen and Blackwelder,[4] the boundary layer is Blasius-like for at least the first 10 cm. Since the purpose of the suction is to reduce or eliminate the low-speed region that results from the streamwise vortices, the suction holes at $x = 40$ cm try to reverse the effects of the previous 30 cm. Consequently, an effective streamwise suction length of 30 cm was used. Since the average spanwise spacing between low-speed regions is 3.2 cm, the effective suction area A_E is 96 cm^2.

Results and Discussion

Figure 2 depicts the experimental situation. Because of the updraft action between pairs of counter-rotating streamwise vortices removing low-momentum fluid away from the wall, an inflectional velocity profile results in both the normal and spanwise directions. When particulates such as smoke are introduced into this vortical flow system, the smoke coalesces to the low-speed region resulting in a streak-like visual pattern. Downstream, this low-speed streak develops a secondary instability and then breaks down. The suction is applied in this experiment to reduce the instability and delay the breakdown of the low-speed streak. Although many different suction rates were tested, results for three suction coefficients of $C_S = 2.4 \times 10^{-5}$ (optimum), 7.2×10^{-5} (moderate), and 20×10^{-5} (large) are presented in detail. In comparison, the amount of suction (i.e., C_S or Q_S) required for the asymptotic profile[2,7] over a comparable area is more than an order of magnitude larger (see Table 1). It should be noted, however, that this comparison with asymptotic suction should be done with care. In asymptotic suction, the purpose is to maintain laminar flow, and the method used is uniform suction; this is quite different from pointwise suction. As discussed earlier, the velocity through the wall V_w is larger for pointwise suction since the hole diameter (i.e., actual suction area) is small. Although this

Table 1 Suction conditions

Case	$C_S \times 10^{-5}$	Q_S, cm^3/s	V_w/U_∞
Optimum	2.4	1.2[a]	0.29
Moderate	7.2	3.5[a]	0.88
Large	20	9.6[a]	2.44
Asymptotic	300[b]	144[b]	0.003

[a]For an effective suction area of 96 cm^2 which is necessary to affect one typical low-speed streak.
[b]Based on an assumption of comparable effective area.

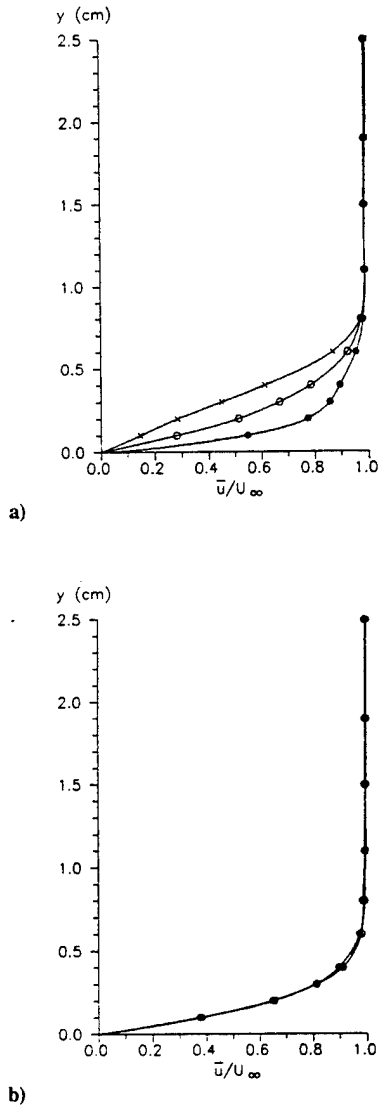

Fig. 3 Time-averaged velocity profile in the normal direction at x = 80 cm for pointwise suction applied at x = 40 cm, z = 8.2 cm; × no suction, ○ $C_S = 7.2 \times 10^{-5}$, ● $C_S = 20 \times 10^{-5}$: a) profile over the low-speed region, z = 8.2 cm and b) profile over the high-speed region, z = 7.0 cm.

suction velocity through the wall may be relatively large locally, the overall suction rates (e.g., Q_S) necessary to affect a given area is much smaller since suction is applied selectively. Measurements were not taken in the immediate vicinity of the suction holes, but farther downstream since the purpose of the present experiment is to determine the effect of selective suction on the breakdown of the low-speed streaks.

Figure 3 shows the velocity profile in the normal direction at spanwise locations over the low- and high-speed regions. The velocity profile for the no suction case in Fig. 3a is inflectional and unstable. When suction is applied, the profile becomes fuller and, therefore, more stable. Although normal profile measurements for optimum suction ($C_S = 2.4 \times 10^{-5}$) were not taken, the missing velocity profile should fall between the no suction and moderate suction cases. Since the suction is applied pointwise in this experiment, the effect of suction is not felt in the high-speed region shown in Fig. 3b, and these profiles remain virtually unchanged.

The smoke wire flow-visualization results, with and without suction, are shown in Fig. 4. Each photograph encompasses a spanwise region including seven low-speed streaks (although the streak at $z = -0.6$ cm is somewhat obscured by the reference centerline). Suction was applied upstream at $x = 40$ cm under these low-speed streaks (and two others outside the photographic field of view). For the no suction case in Fig. 4a, the low-speed streaks develop a sinuous motion instability starting from about $x \approx 115$ cm.

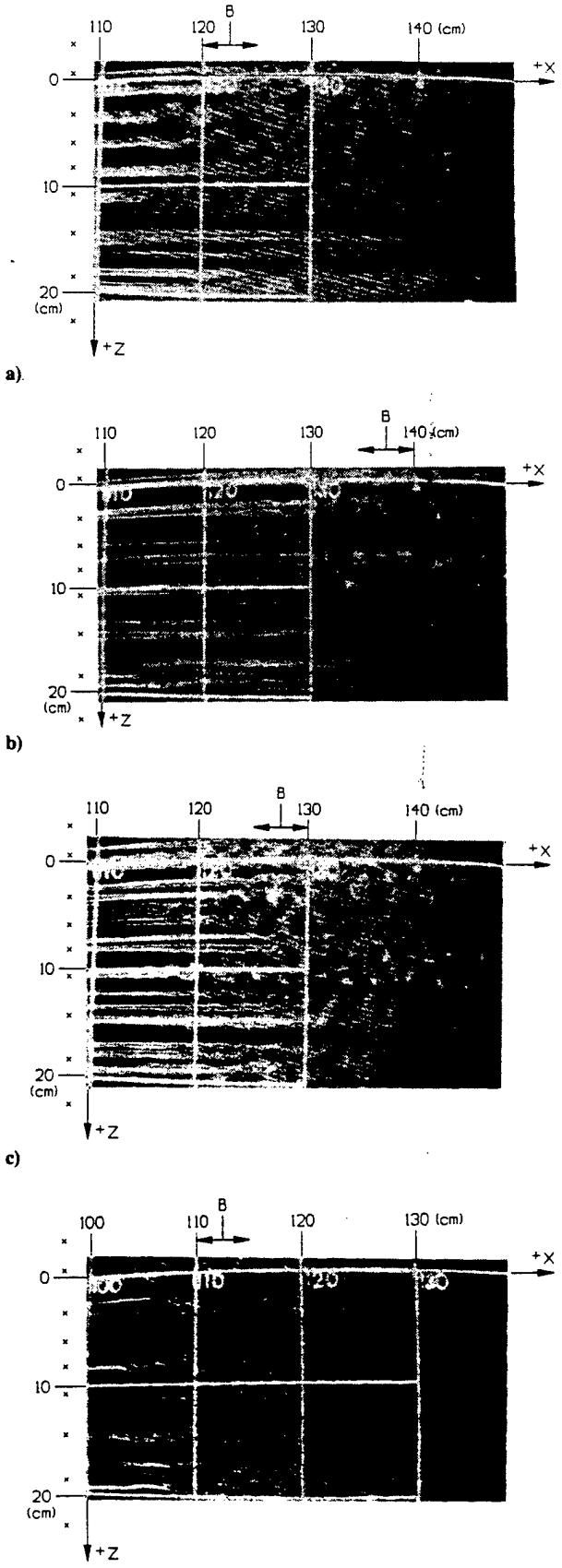

Fig. 4 Smoke wire flow visualization with and without suction, flow direction left to right, horizontal and vertical white reference lines 10 cm apart, suction holes (at z = −3.3, −0.6, 3.3, 5.9, 8.2, 10.7, 14.4, 18.5, and 22.7 cm) indicated by ×. Although hole locations are shown in a), no suction was applied in this case; typical breakdown location for the five upper streaks [i.e., those in the range $-0.6 \leq z$ (cm) ≤ 10.7] is indicated by B: a) no suction case, b) $C_S = 2.4 \times 10^{-5}$, c) $C_S = 7.2 \times 10^{-5}$, and d) $C_S = 20 \times 10^{-5}$.

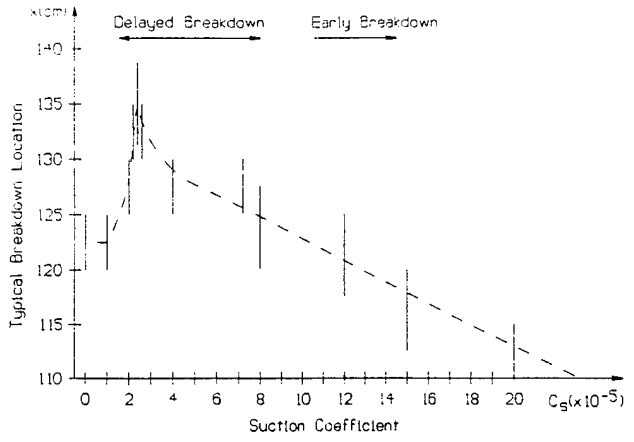

Fig. 5 Typical breakdown location as a function of suction coefficient.

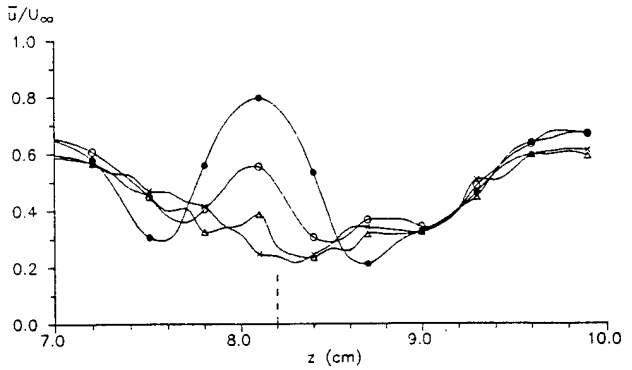

Fig. 6 Time-averaged velocity profile in the spanwise direction at x = 80 cm, y = 0.2 cm, pointwise suction is applied at x = 40 cm, z = 8.2 cm (indicated by the dashed lines); ×, no suction, △ $C_S = 2.4 \times 10^{-5}$, ○ $C_S = 7.2 \times 10^{-5}$, and • $C_S = 20 \times 10^{-5}$.

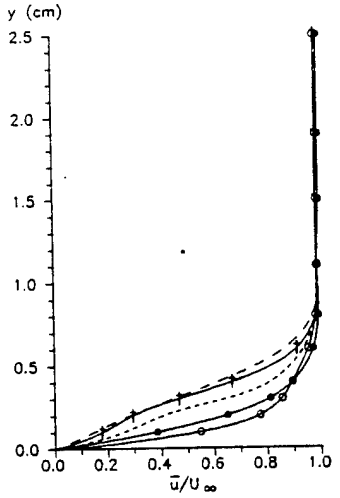

Fig. 7 Time-averaged velocity profile in the normal direction at x = 80 cm. Although not explicity shown, the velocity profile at the high-speed region for the no suction case is quite similar to the velocity profile at z = 7.0 cm for the large suction case (as shown in Fig. 3b): no suction — — low-speed region, z = 8.2 cm and - - - - mid-speed region, z = 7.6 cm; $C_S = 20 \times 10^{-5}$, large suction ○ at z = 8.2 cm, † at z = 7.6 cm, and • at z = 7.0 cm.

This instability leads to the breakdown of the low-speed streaks by $x \approx 120$–125 cm. For the optimum suction case shown in Fig. 4b, the sinuous motion instability is delayed until $x \approx 125$–130 cm, and breakdown does not occur until $x \approx 135$–140 cm. This delaying effect is especially significant in light of the fact that the applied suction rate is extremely small, i.e., about two orders of magnitude smaller than the suction rate required for an asymptotic profile. At a moderate suction rate shown in Fig. 4c, there is a delay of about 5 cm (compared to the no suction case) for the onset of sinuous motion instability and breakdown of the low-speed streak. This is not as significant a delay as the optimum suction case. A closer examination of the flow-visualization results reveal that the smoke in the center of individual low-speed streaks is often nonexistent. The low-speed streaks at $z \approx 3$ cm and 8 cm in Fig. 4c, for example, have dark smokeless center regions when compared to the same low-speed streaks in Fig. 4a. The smokeless regions may be due to smoke removal by the suction ports. Another possibility is the presence of a local high-speed region since the smoke tends to coalesce in low-speed regions. In Fig. 4d, the photographic field of view shown is 10 cm upstream of the other flow-visualization photographs. It is evident that the high-suction rate has precipitated a premature breakdown of the low-speed streaks. A closer examination of the flow-visualization results for the higher suction rates indicate that the number of low-speed streaks has doubled over the spanwise region where suction was applied as discussed later on.

Figure 5 summarizes the effect of suction rate on the breakdown of the low-speed streaks. These results are based on flow visualizations similar to those shown in Fig. 4. For each suction rate, the range of breakdown locations observed during multiple flow-visualization runs are shown in Fig. 5. A consistent trend in the low-speed streak breakdown location is shown by the figure. The breakdown is delayed farther downstream as the suction rate is increased from zero up through the optimum suction rate of $C_S = 2.4 \times 10^{-5}$. However, as the suction rate is increased beyond optimum, breakdown begins to move upstream. The reason for this early breakdown becomes apparent when the spanwise velocity profile is examined.

The velocity profile in the spanwise direction for the four different cases are shown in Fig. 6. The no suction case indicates that the low-speed streak is centered at about $z \approx 8.2$ cm. It is evident from the figure that pointwise suction produces a higher speed flow where a low-speed region existed in the no suction case. At moderate suction rate, this higher speed flow at $z = 8.2$ cm is strong enough to locally impede the coalescence of smoke particulates near the streak center as shown in Fig. 4c. The optimum and moderate suction rate cases produce the higher speed flow in the immediate vicinity of the suction hole without significantly affecting other spanwise regions. At the high-suction rate, the velocity at $z = 8.2$ cm is higher speed than even the archetypical high-speed regions at $z = 7$ cm and $z \approx 10$ cm. Furthermore, the midspan regions of $z = 7.6$ and 8.7 cm are transformed into low-speed regions with velocities comparable to the no suction case low-speed region. Consequently, for the high-suction rate case, there are twice as many low-speed regions, and the spacing between low-speed streaks (as well as the Görtler vortex wavelength) has thus been halved. Myose and Blackwelder[9] found that a reduction in the Görtler vortex wavelength resulted in early onset of secondary instability and breakdown of the low-speed streaks. Both the wavelength halving and the early breakdown are consistent with the flow-visualization result of Fig. 4d.

A further comparison between the high-suction rate and no suction cases are presented in Fig. 7. High suction transforms the inflectional profile at $z = 8.2$ cm (long dashed line) into a profile (○) which is fuller than the archetypical high-speed region at $z = 7.0$ cm (•). In the midspan region ($z = 7.6$ cm), high suction results in a profile (†) which is more inflectional than the profile in the low-speed region of the no suction case (long dashed line). Swearingen and Blackwelder[4] found that the normal profile became more inflectional in the low-speed region and fuller in the high-speed region as the flow developed downstream and became unstable. This suggests that the flow is highly unstable at high-suction rate. Figure 6 also indicates that spanwise shear ($\partial U/\partial z$) in the profile at high-suction rate is significantly larger than the no suction case. Swearingen and Blackwelder[4] found that inflectional spanwise profiles and large spanwise shear cause flow instability just as inflectional normal profiles do. Therefore, the flow is actually made more unstable when suction is applied at too high a rate. When selective suction is properly applied as in the optimum and moderate suction cases, a fuller, more stable profile is produced in the normal direction

whereas in the spanwise direction the velocity difference between low- and high-speed regions are diminished. In such a case, the onset of sinuous instability and breakdown of the low-speed streak is delayed as illustrated in Fig. 4.

Additional suction methods were attempted to try and obtain further delays in the onset of instability and breakdown. These attempts included the use of larger 0.3-cm-diam holes (at $x = 41$ cm), increasing the number of suction holes from 9 to 27 (0.1 cm diameter at $x = 30$, 40, and 55 cm), and employing a plenum system of 72 holes (0.1 cm diameter at 5-cm intervals between $x = 35$ and 70 cm); however, suction was still applied only under the low-speed streaks. These methods were employed with the idea that suction would be applied more gently and over a longer downstream distance. None of these methods resulted in further delays of breakdown onset. Since the low-speed streak is located directly above the suction port (see Fig. 2), the effect of suction will be felt more strongly in the normal direction than in the spanwise direction. To reduce the spanwise velocity difference between the high- and low-speed regions and, hence, reduce the spanwise inflectional profile, additional suction ports would need to be employed with a spanwise displacement. This application of selective suction would alleviate the additional spanwise inflection points introduced by the strong suction (see Fig. 6) and possibly delay the breakdown farther downstream. An alternative approach would be to apply suction in the low-speed region and injection in the high-speed region as suggested by Gad-el-Hak and Blackwelder.[8] Neither of these methods was attempted during the course of this experiment.

Conclusions

Selective suction has a significant effect upon the low-speed regions and their breakdown according to the present experiment. Results indicate that suction should be applied in such a manner that a more stable fuller profile is promoted in the normal direction without generating an additional instability in the spanwise direction. Consequently, an ideal control method should produce a fuller profile in the normal direction and eliminate the difference between low- and high-speed regions in the spanwise direction. At optimum suction rates, selective suction successfully delayed the breakdown of the low-speed region, and by analogy should reduce the production of turbulent energy in a turbulent boundary layer. The main conclusion from this study is that the suction rate necessary for delay of breakdown was significantly reduced (by about two orders of magnitude) by selective application of suction at judiciously chosen spanwise locations.

Acknowledgments

This work was sponsored by the Office of Naval Research under Contract N00014-92-J1062 monitored by L. P. Purtell. This support is gratefully acknowledged. The authors acknowledge the assistance of Depei Liu for the pressure gradient information of the Görtler wind tunnel.

References

[1]Whites, R. C., Suddereth, R. W., and Wheldon, W. G., "Laminar Flow Control on the X-21," *Astronautics and Aeronautics*, Vol. 4, July 1966, pp. 38–43.

[2]Schlichting, H., *Boundary-Layer Theory*, 7th ed., McGraw–Hill, New York, 1979, pp. 383–388, 506–510.

[3]Robinson, S. K., "Coherent Motions in the Turbulent Boundary Layer," *Annual Review of Fluid Mechanics*, Vol. 23, 1991, pp. 601–639.

[4]Swearingen, J. D., and Blackwelder, R. F., "The Growth and Breakdown of Streamwise Vortices in the Presence of a Wall," *Journal of Fluid Mechanics*, Vol. 182, Sept. 1987, pp. 255–290.

[5]Blackwelder, R. F., "Some Ideas on the Control of Near-Wall Eddies," AIAA Paper 89-1009, March 1989.

[6]Johansen, J. B., and Smith, C. R., "Effects of Cylindrical Surface Modifications on Turbulent Boundary Layers," *AIAA Journal*, Vol. 24, No. 7, 1986, pp. 1081–1087.

[7]Roon, J. B., and Blackwelder, R. F., "The Effects of Longitudinal Roughness Elements and Local Suction upon the Turbulent Boundary Layer," *Structure of Turbulence and Drag Reduction*, edited by A. Gyr, Springer–Verlag, Zurich, 1990.

[8]Gad-el-Hak, M., and Blackwelder, R. F., "Selective Suction for Controlling Bursting Events in a Boundary Layer," *AIAA Journal*, Vol. 27, No. 3, 1989, pp. 308–314.

[9]Myose, R. Y., and Blackwelder, R. F., "Controlling the Spacing of Streamwise Vortices on Concave Walls," *AIAA Journal*, Vol. 29, No. 11, 1991, pp. 1901–1905.

FED-Vol. 193, Turbulence Control
ASME 1994

DELAY OF BREAK-DOWN OF STREAMWISE VORTICES EMBEDDED IN A BOUNDARY LAYER

Ron F. Blackwelder and Depei Liu
Department of Aerospace Engineering
University of Southern California
Los Angeles, California

Abstract

The delay of the break-down of counter-rotating streamwise vortices generated by a Görtler instability in a boundary layer on a concave wall was studied. The vortices were subjected to a small amplitude excitation produced by a delta wing positioned on the wall in a low speed region so that it sheds vortices opposite in sign to that of the Görtler system. Smoke wire visualization and hot-wire measurements have been made downstream for a variety of oscillation modes. Results show that a very small amplitude oscillation is sufficient to reduce the spanwise shear and delay the break-down of the streamwise vortices. The spanwise shear plays a more prominent role in the transition to turbulence than the vertical shear which is consistent with the results of Swearingen & Blackwelder(1987).

Introduction

The growth and break-down of streamwise vortices in the presence of a concave wall was recently investigated experimentally by Swearingen & Blackwelder (1987). They found that the development of Görtler vortices can be divided into five stages: receptivity, Görtler linear instability and amplification, secondary instability, nonlinear amplification and breakdown. The first stage, receptivity, was concerned with how the environmental disturbances, such as free-stream perturbations and wall roughness, were coupled with the boundary layer to produce growing disturbances in the flow over a concave wall. The second stage, linear instability, produced the well known linear growth of the Görtler streamwise vortices. These streamwise vortices do not cause transition by themselves but

they set up a flow field that was unstable to other disturbances leading to the secondary instability stage which produce higher growth rates. These disturbances rapidly become nonlinear and lead to the break-down stage. It was found that the streamwise velocity became inflectional both in the spanwise direction and vertical direction. However the inflectional shear layer developed much earlier in the spanwise direction than the vertical direction. Consequently the spanwise shear was more closely correlated with the maximum fluctuating streamwise velocity than the vertical shear.

On the theoretical side, Hall & Seddougui (1989) have investigated the onset of three-dimensionality and time-dependence in Görtler vortices. They showed that the flow field can be divided into five layers with the vortex activity confined to the mid region of the boundary layer. The secondary instabilities are confined to small shear layers adjoining the vortices. The vortex activity grows as the flow moves downstream until it eventually occupies almost all of the boundary layer.

Blackwelder (1983) studied the analogy between transitional and turbulent boundary layer and found many similarities between the two flows. The first similarity is the existence of streamwise vortices in each flow field. These vortices were argued to be responsible for elongated low speed regions appearing at their side in both flows. The low speed streaks was concomitant with the development of the spanwise inflectional velocity profiles in the low speed regions due to the streamwise vortices in both of the flow fields. An additional similarity is the break down of the streamwise vortices which cause the flow transition to turbulence in the transitional flow or produced the turbulence in the fully developed flow field. He also pointed out that the streamwise vortices play a very important role in the production of turbulent energy in turbulent boundary layer. For this reasons, if the stream vortices in the Görtler flow can be controlled, knowledge of the controlling techniques will be very useful in understanding how to control the turbulent boundary layer.

Thus this work was undertaken to determine the susceptibility of streamwise vortices to small amplitude excitations with the goal of delaying the break-down of the vortices.

Experimental Conditions

The experiments were conducted in the University of Southern California Görtler wind tunnel described in detail by Swearingen & Blackwelder (1987). The concave test plate has a span of 1.2m, is 2.4m long, and has a radius of curvature of 3.0m. The freestream u' turbulence level was less than 0.07% and spanwise deviations in the free stream velocity along the spanwise direction were less than 0.5% across the test section.

The excitation system for introducing the controlling vortices into the flow is shown in Figure 1. The primary component was a small delta wing made of spring steel (C-1095, product of Lyon Industries). The leading edge was swept 75° back from the

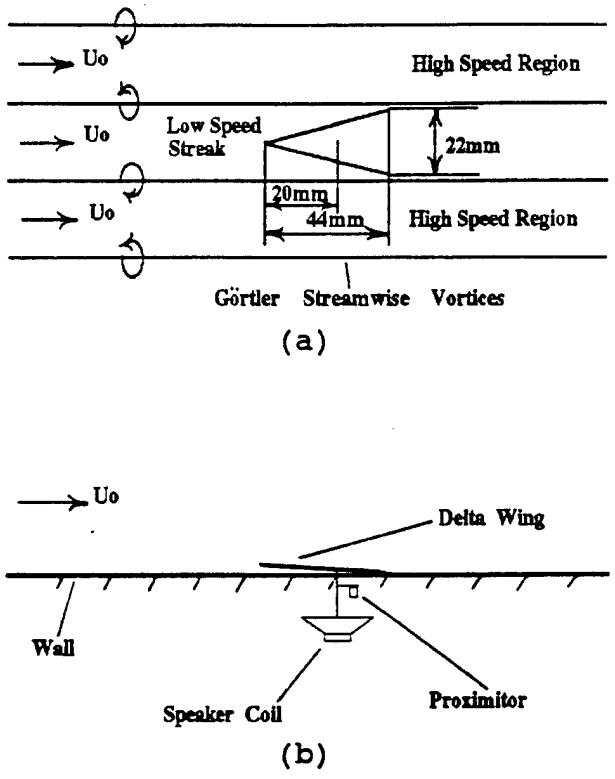

Figure 1. Schematic of excitation system, (a) plan view, (b) side view.

mean flow. It had a chord of 44 mm and a thickness 0.1mm. The spanwise length of 22 mm was approximately the distance between the naturally occurring Görtler stationary vortices. The delta wing was mounted flush with the wall at a streamwise location 38cm from the leading edge. To produce stream-wise vortices opposite in sign to the existing ones, the delta wing was placed in the low speed region of fluid. It was excited by a speaker coil located on the non-working side of the convex plate and connected to the delta wing by a small shaft attached 20 mm down-stream of the its apex. The speaker was driven by an oscillator which controlled its frequency and amplitude. The trailing edge of the delta wing was permanently attached to the concave plate by tape so that the excitations moved the delta wing from a zero angle of attack to some finite value and back to zero. The amplitude of the oscillation was measured by a Bently Nevada proximitor gage, model 3000, shown in figure 1.

The streamwise velocity was measured by a single hot-wire probe described by Swearing and Blackwelder(1987). The probe was located 1.20 m downstream of the leading edge of the concave wall. It was mounted on a traverse controlled by a PC computer which could move the probe in the spanwise and normal directions. The accuracies in the normal and spanwise directions were 0.02 mm and 0.05 mm respectively. The unfiltered signals were sampled by RC Electronics ISC-16 analog-to-digital converters which were controlled by the computer. The analog to digital converters had a maximum throughput of 500 khz per channel. An actual digitizing rate of 1000 samples/sec was used and the digitized samples were then stored on a hard disk.

A smoke wire was used to visualize the low speed streaks and their subsequent break down. It was mounted 1.0 mm from the wall parallel to the test plate. It was oriented vertically along the spanwise direction so that the oil droplets could flow along the wire via gravity. The wire heating was controlled by a home made timing circuit. Best visualization was obtained when it was placed at x = 60cm from the leading edge of the concave wall.

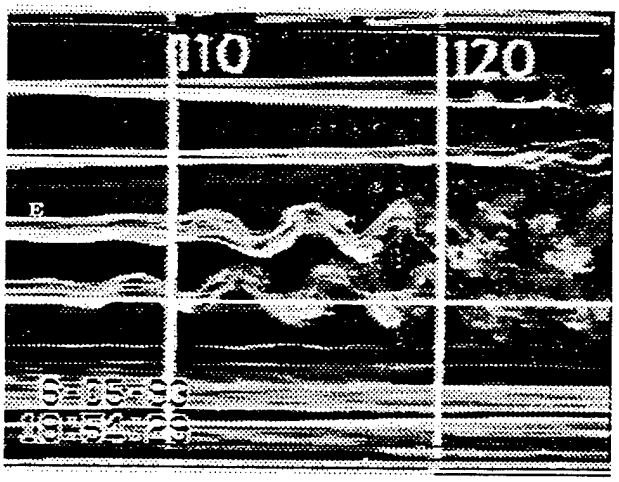

Figure 2. Flow Visualization without excitation. The delta wing exciter is located at x = 38 cm and z = 2.5cm under the low speed region denoted by 'E.'

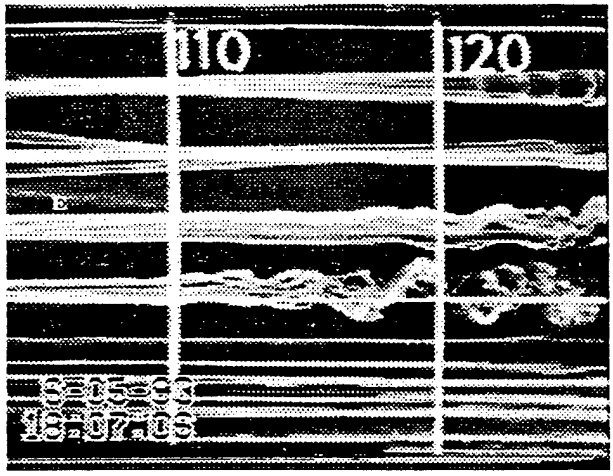

Figure 3. Flow visualization of the same flow field as in figure 2 but with the delta wing oscillating at f = 100 Hz with an amplitude of 0.1mm.

Results and Discussions

A visualization of the low speed regions between the undisturbed Görtler vortices is shown in figure 2 for the region 104 to 126 cm downstream of the leading edge of the concave plate. The flow is from left to right and roughly five low speed regions filled with smoke are shown. Two of the streaks in the middle of the photo are seen to be in the process of transition from a laminar state to a turbulent one. Their natural oscillations have a wave length of approximately 3cm and a frequency of roughly 110Hz. The delta wing actuator is located upstream under the streak marked by 'E.' It was installed but not excited during the filming of figure 2. Figure 3 shows the same flow region but with the delta wing oscillating at 100Hz and an amplitude of 0.10mm. As seen in the figure, the oscillation and transition of the 'E' streak have been delayed at least 10cm downstream.

Figure 4 shows measurements of the mean streamwise velocity as a function of the spanwise direction. For this data, the hot-wire probe was traversed in the spanwise direction at a distance of 16 mm from the wall. This location is in the outer region of the boundary layer and the velocity fluctuations in the low speed region were a maximum there. The magnitude of the velocity deficit in the low speed region was always reduced by the excitation as seen in the figure. Not only is the deficit reduced by the excitation, but the region, and thus extent, of the strong spanwise shear is reduced. The corresponding decrease in the streamwise velocity fluctuations

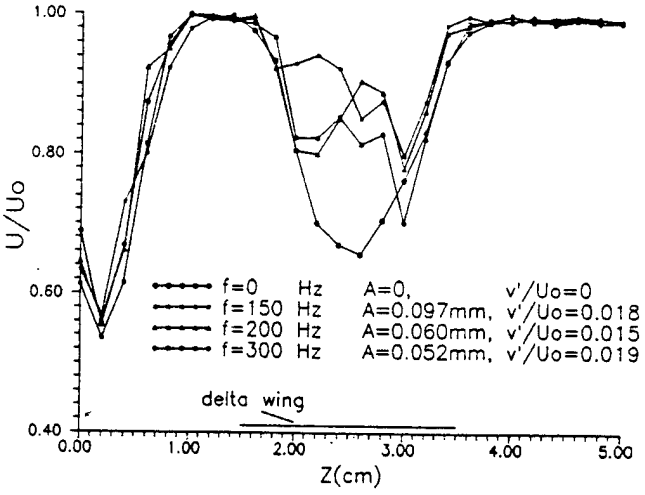

Figure 4. Spanwise velocity profile at y = 16mm.

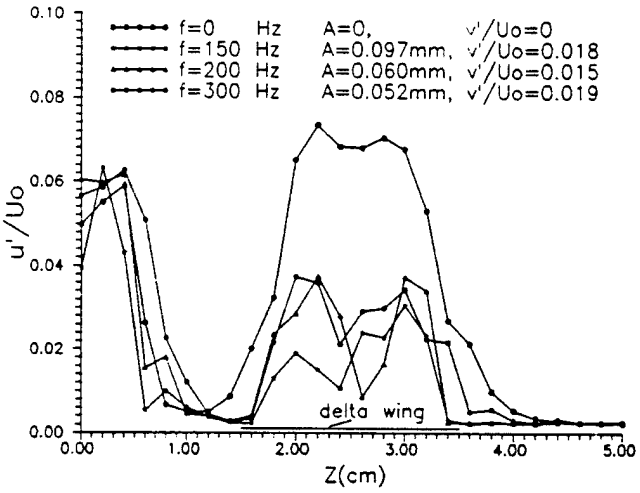

Figure 5. The fluctuating velocity profiles at y = 16mm.

is found in figure 5. It is clear from these two figures that only a very small amplitude oscillation is sufficient to have a strong and remarkable effect on the transitional boundary layers.

The effect of the excitation amplitude on the normal velocity profile is shown in figure 6 for a constant frequency of 100 Hz. As the amplitude increased, the mean velocity gradient in the upper region increased. Thus although the spanwise shear was reduced in figure 4, the vertical shear increased. Since the spanwise shear was reduced and the breakdown moved downstream when the perturbation was turned on, this suggests that the breakdown was due to the spanwise shear and not to the vertical shear, in agreement with the results obtained by Swearingen & Blackwelder (1987). There was a small change in the mean U(y) velocity profile when the oscillation amplitude increased from zero to 0.092mm. However, a much larger effect was observed when the excitation amplitude increased further to 0.1mm. It was surprising that the thin shear layer was very sensitive to the excitation amplitude after the amplitude increased beyond some critical point. This non-linearity was observed in several of the measurements and is presently unexplained. The mean velocity below the strong shear region was almost constant for the three amplitudes of oscillation. Figure 7 shows the streamwise velocity fluctuations corresponding to figure 6. The maximum fluctuation was dramatically reduced for amplitudes exceeding 0.092mm.

Figure 8 presents the mean velocity profiles in the vertical direction at varying amplitudes and frequencies. At each frequency, the amplitude was chosen to yield a nearly constant

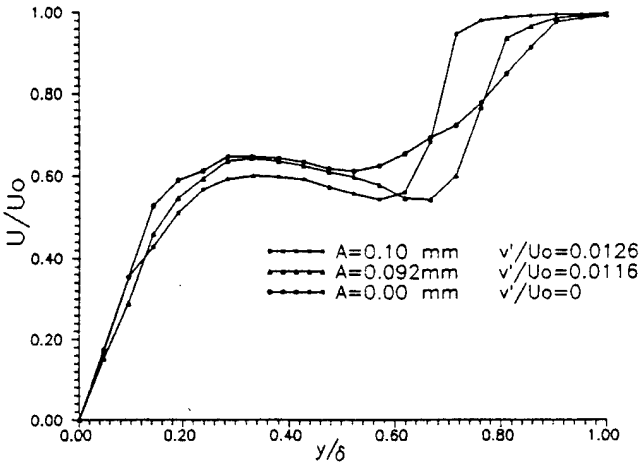

Figure 6.Mean velocity profiles for x = 2.4 cm and f = 100Hz.

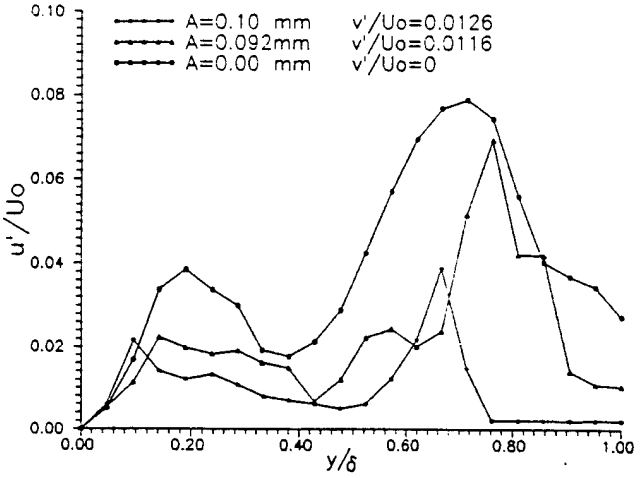

Figure 7.RMS velocity profiles corresponding to the flow in figure 6.

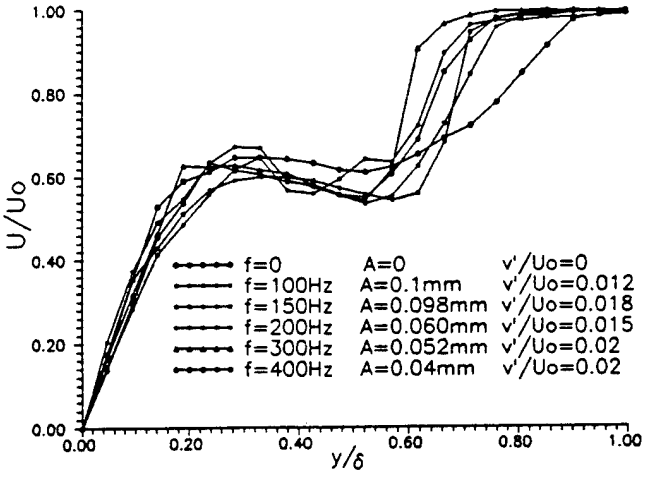

Figure 8. Mean velocity profiles normal to the wall at z = 2.4 cm.

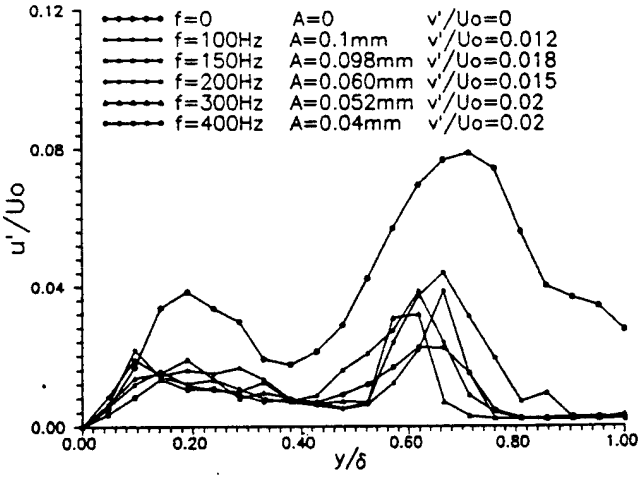

Figure 9. RMS velocity profiles in the normal direction at z = 2.4 cm.

fluctuation value of $0.03 \cdot U_\infty$ at the location of the strong shear; i.e. at $0.6 < y/\delta < 0.7$. as shown in figure 9. For frequencies from 100 Hz to 400 Hz, this procedure successfully reduced the maximum normalized fluctuation velocity from 0.08 to about 0.03 - 0.04 as seen in figure 9. For all above cases, the mean spanwise velocity deficit was reduced in the upper regions of the boundary layer(not shown), but the spanwise profiles were almost constant below this region.

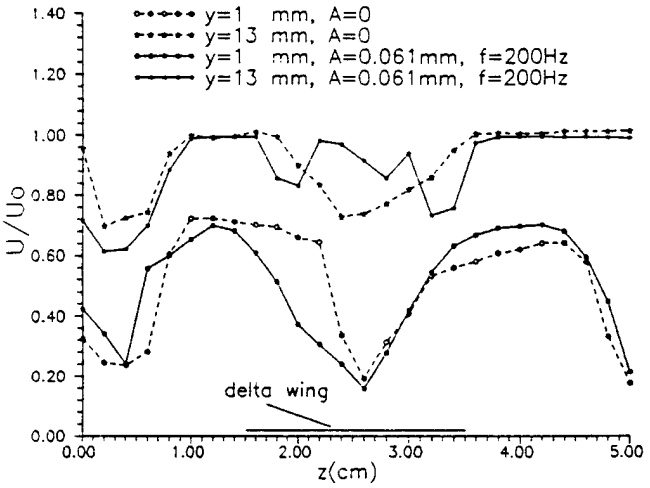

Figure 10. Mean velocity profiles at x = 1.2m

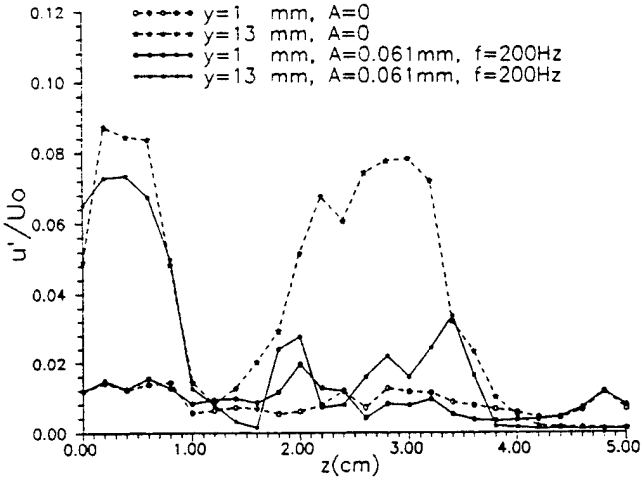

Figure 11. RMS velocity profiles at x = 1.2 m.

Figure 10 compares the changes of the mean velocity profiles in the spanwise direction in the upper and lower regions of the boundary layer with and without excitation. The corresponding velocity fluctuations are shown in figure 11. At the lower level, the excitation did not cause much change in the mean velocity nor the fluctuation velocity. However, the excitation causes significant change for both the mean and fluctuation velocity at the upper layer. The above measurements (including figure 4 to figure 11) indicated that the secondary instability occurs at the upper thin shear layer. In addition, the small amplitude excitation mainly changed the spanwise shear in the upper region. This change appears to delay the secondary instability which is consisted with the results of Hall & Seddougui (1989).

Figure 12 shows the amplitude required to reduce the maximum fluctuation velocity from 0.08 to about 0.04 at different frequencies of excitation. The figure indicates that for the higher frequencies, smaller excitation amplitude are needed. The scale on the right hand side shows that the required amplitudes

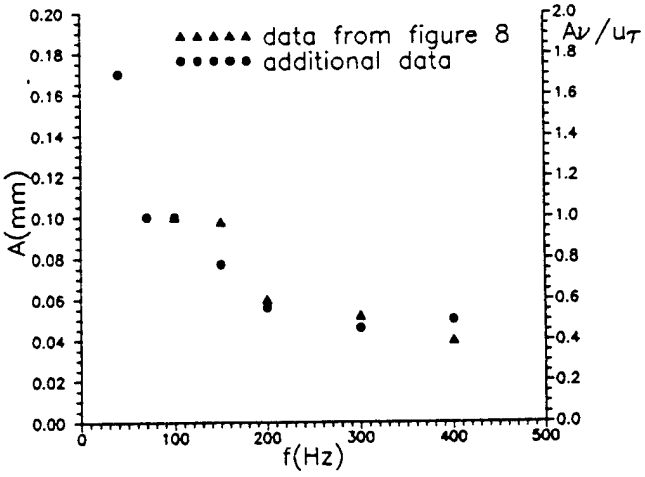

Figure 12. The relationship between excitation the amplitude and the frequency.

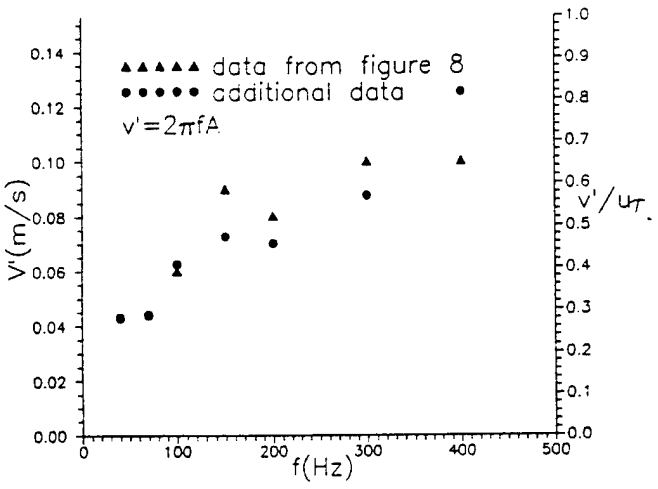

Figure 13. The relationship between the disturbance velocity and the frequency.

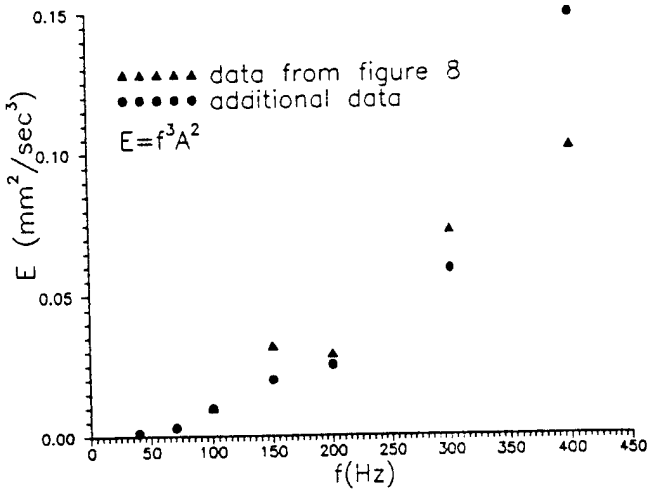

Figure 14.The relationship between the energy and the frequency.

are comparable to the viscous scale in the boundary layer, ν/u_τ, where u_τ is the friction velocity. The friction velocity, u_τ, was calculated assuming a Blasius boundary layer (see Blackwelder 1983) by

$$\frac{u_\tau}{U_\infty} = 0.576 \cdot Re_x^{-1/4}$$

Figure 13 presents the relationship between amplitude of the disturbance velocity and the frequency of oscillation required to reduce the fluctuation velocity at x = 1.20m by 50%. This data corresponds to the data in figure 12. The disturbance velocity was calculated by $v' = 2\pi \cdot A \cdot f$ where A is the amplitude and f is the frequency of the oscillation. The higher the frequency, the larger the disturbance velocity needed. Note the right hand scale shows that the velocity of the delta wing is of the order of the friction velocity in the boundary layer.

For the active control, the power required to execute the control is one of the more important parameters. Figure 14 illustrates how a measure of the power obtained by A^2f^3 increases as the frequency of the perturbation increases. Hence it would appear that it would be more desirable to operate the actuator at the lower frequencies.

Discussion and Conclusions

The above results indicate that the break-down of streamwise vortices embedded in a laminar boundary layer was delayed only when the mean velocity in the upper region of the boundary layer was changed. The delta wing was mounted flush with the wall and had a maximum amplitude of 1 to $2\nu/u_\tau$. Thus disturbances generated at the wall were definitely influencing the flow in the outer regions of the boundary layer. If the disturbances had been pressure disturbances, their effect would

most likely have been largest near the point of excitation and would have affected the flow field further upstream. Thus it is felt that the pressure perturbation associated with the disturbances are not as important as the vortical perturbations. Since delta wings are known to generate counter-rotating trailing vortices, this type of a disturbance seems to be the most predominate. Hence, the perturbing vortices must migrate from the wall outward to affect the outer region of the boundary layer.

A simplified model of the interaction seems elusive at this time since the disturbance vortices are generated in a strongly viscous region. The induced flow of the Görtler vortices will move the pair of disturbance vortices toward each other and away from the wall as shown in figure 15. On the other hand, the interaction of the delta wing vortices with themselves will tend to move each other toward the wall. Thus a larger amplitude of the disturbance vortices would tend to inhibit their outward migration. Counter balancing this effect is the viscous decay. As the disturbance vortices move downstream, they will decay, especially while in the viscous region of the boundary layer near the wall. Thus the effects reaching the outer region of the boundary layer will depend upon a nonlinear viscous interaction of both sets of vortices. In addition, the diameters and length scales of the vortices will also affect the results. Thus one conclusion is that the movement of the disturbance vortices must depend upon the relative location and strengths of the different sets of the vortices. This may help explain the non-linearity encountered in the amplitude of the disturbance.

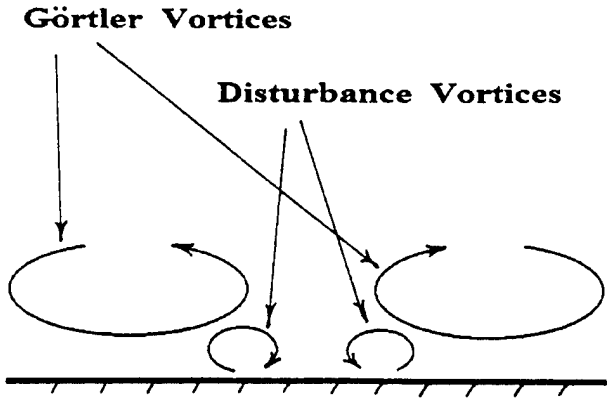

Figure 15. The relative position of the disturbance vortices and the Görtler vortices.

Another question arising in this investigation concerns the need for the unsteadiness of the disturbance vortices. At first thought, it would appear that a steady set of vortices of comparable amplitude would be as effective in delaying the breakdowns of the Görtler system. However when the delta wing was set at a constant angle of attack at amplitudes comparable to those in Figures 9, 11, 12, etc., the flow downstream did not display a large change and transition remained in the same relative position. As the angle of attack of the delta wing continued to increase, the transition point suddenly moved upstream when the amplitude was approximately 2mm. Evidently the steady disturbance had little effect on the breakdown until it was so large that it acted more like a traditional roughness element. On the other hand, the actuator was most

effective in reducing the velocity fluctuations downstream when it was oscillated near the fundamental frequency(or a harmonic thereof) of the natural oscillations seen in figure 2. This effect is being studied further.

Thus in conclusion, the smoke wire visualization and the hot-wire data have both showed that a significant delay of the breakdown of streamwise vortices embedded in a boundary layer can be achieved by a very small amplitude excitation. The secondary instability preceding breakdown can be delayed only when the disturbance vortices exceed some critical amplitude and have moved away from the wall. The spanwise shear plays a more prominent role in the transition to turbulence than the vertical shear which is consistent with the earlier results of Swearingen & Blackwelder.

Acknowledgements

The authors thank the Office of Naval Research for their continuing support of this research under Contract N00014-92-J-1062 monitored by Dr. Pat Purtell. We also acknowledge Professor Fred Browand's interest and suggestions in this work.

References

Blackwelder, R.F., 1983, "Analogies between transitional and turbulent boundary layers," Phy. Fluids, 26, 2807.

Hall,P. & Seddougui,S., 1989, "On the onset of three-dimensionality and time-dependence in Görtler vortices," J. Fluid Mech. 204, 405

Swearingen, J.D. & Blackwelder, R.F., 1987, "The growth and breakdown of streamwise vortices in the presence of a wall," J. Fluid Mech., 182, 255.